arXiv:0906.2360v1 [astro-ph.SR] 12 Jun 2009

Astronomical Journal, in press

HOT SUBDWARF STARS AMONG THE OBJECTS REJECTED FROM THE PG CATALOG: A FIRST ASSESSMENT USING GALEX PHOTOMETRY

Richard A. Wade and M. A. Stark

Department of Astronomy and Astrophysics, The Pennsylvania State University, 525 Davey Lab, University Park, PA 16802

wade@astro.psu.edu, stark@astro.psu.edu

Richard F. Green

Large Binocular Telescope Observatory, University of Arizona, 933 N. Cherry Ave., Tucson, AZ 85721-0065

rgreen@as.arizona.edu

Patrick R. Durrell

Department of Physics and Astronomy, Youngstown State University, Youngstown, OH

prdurrell@ysu.edu

ABSTRACT

The hot subdwarf (sd) stars in the Palomar Green (PG) catalog of ultraviolet excess (UVX) objects play a key role in investigations of the frequency and types of binary companions and the distribution of orbital periods. These are important for establishing whether and by which channels the sd stars arise from interactions in close binary systems. It has been suggested that the list of PG sd stars is biased by the exclusion of many stars in binaries, whose spectra show the Ca II K line in absorption. A total of 1125 objects that were photometrically selected as candidates were ultimately rejected from the final PG catalog using this K–line criterion. We study 88 of these "PG–Rejects" (PGRs), to assess whether there are significant numbers of unrecognized sd stars in binaries among the PGR objects. The presence of a sd should cause a large UVX, compared with the cool K–line star. We assemble GALEX, Johnson V, and 2MASS photometry

and compare the colors of these PGR objects with those of known sd stars, cool single stars, and hot+cool binaries. Sixteen PGRs were detected in both the far– and near–ultraviolet GALEX passbands. Eleven of these, plus the 72 cases with only an upper limit in the far–ultraviolet band, are interpreted as single cool stars, appropriately rejected by the PG spectroscopy. Of the remaining five stars, three are consistent with being sd stars paired with a cool main sequence companion, while two may be single stars or composite systems of another type. We discuss the implications of these findings for the 1125 PGR objects as a whole. An enlarged study is desirable to increase confidence in these first results and to identify individual sd+cool binaries or other composites for follow–up study. The GALEX AIS data have sufficient sensitivity to carry out this larger study.

Subject headings: binaries: close - stars: horizontal-branch - subdwarfs - ultraviolet: stars

1. INTRODUCTION

The subdwarf B (sdB) stars are the field analog of cluster stars lying on the Extended Horizontal Branch (EHB), with 18000 K $\lesssim T_{\rm eff} \lesssim$ 30000 K and $\log g \approx 5.5 - 6$. Some subdwarf O (sdO) stars form an extension of the EHB to higher temperatures. We will refer to these two groups together simply as "hot subdwarf" (sd) stars. These stars may be an important source of ultraviolet (UV) light in early–type galaxies (O'Connell 1999; Brown et al. 2000; Han et al. 2007; Yi 2008), and it is important to understand their origins so that their contribution can be properly estimated.

The sd stars are core He–burning stars, with typical total mass $\sim 0.5 M_\odot$ but only very small H envelopes ($M_H \lesssim 10^{-2}\ M_\odot$) (Saffer et al. 1994). To become a hot subdwarf, a low–mass star must lose its H envelope on its first ascent of the giant branch, within 0.4 mag of the tip (D'Cruz et al. 1996). Since all red giants do not end up on the EHB, some process must enhance the mass loss in stars that do become sd stars. Such a process could be the interaction of the proto–sd star with a close companion star, promoting mass loss either via Roche–lobe overflow (RLOF) or a common envelope (CE). Such a model was first proposed by Mengel et al. (1976), and a much more detailed model has been put forward by Han et al. (2002, 2003), including a population synthesis study. In the Han et al. scenario, the RLOF channels often lead to a sd star paired with an A or early–F companion, the companion's mass being increased by exchange from the proto–sd star. The CE channels usually result in a late–F, G or K dwarf companion (or a white dwarf companion, if the second star to evolve is the one that becomes the sd star at the present epoch). A binary merger channel leading

to isolated sd stars also exists. Thus, an additional reason for determining the evolutionary pathways that lead to sd stars is that they may serve as a calibrating population, to enable the theory of binary mass loss/exchange to be applied more confidently in other contexts.

We have used the 2MASS Point Source Catalog in combination with B, V photometry to study the near infrared (NIR) and optical–NIR colors of a large sample of sd stars (Stark & Wade 2003; Stark et al. 2004). In a volume–limited sample, about 25% of these stars show an infrared excess, suggesting a composite spectral energy distribution. Spectroscopy of a subset of these is consistent with the companions being mostly late–F, G, and K dwarfs (Stark 2005; Stark & Wade 2006). Lisker et al. (2005) also have found late–F, G and K companions to hot subdwarfs, based on $B - J$ color and/or optical spectroscopy. These sd+G/K systems[1] are in accord with one prediction of the binary origin scenario for sd stars. Where are the sd+A/F binaries that Han et al. (2003) also predict? Are the existing catalogs of identified sd stars missing a large number of sd stars in binary systems?

With about 900 hot subdwarfs, the magnitude–limited Palomar Green (PG) catalog of ultraviolet–excess objects (Green et al. 1986) is the dominant contributor to the Kilkenny et al. (1988) catalog of hot subdwarf stars. The PG hot subdwarfs are often the subject of detailed study, either individually or for statistical purposes. The PG candidate sample was constructed from a $U - B$ photographic survey. Candidates showing a Ca II K–line were culled from the final PG catalog, on the supposition that this line indicated the UV excess arose in a relatively cool, metal–poor (Pop II) star with reduced UV line blocking (a subdwarf F/G star: sdF/G)[2], which was not of interest in a survey for quasars and hot stars. Such K–line objects with a modest $U - B$ excess, however, would also describe how an unresolved binary composed of a hot sd star and a cool main sequence (MS) star of type F should appear. A relatively bright F companion would contribute a K–line that is strong enough to be seen in the PG survey spectra (which are of modest signal–to–noise ratio), whereas a typical sd star would dominate over the optical spectrum and colors of a MS G or K companion. Thus it is possible that bona–fide sd+MS binaries, especially those with early–F companions but also late–F, G, or K companions in some cases, are missing from the final PG catalog, although they were selected as *candidates* in the PG survey. Han et al. (2003) noted this possible bias in the PG catalog as an obstacle to confirming their binary formation scenario for hot subdwarf stars, giving it the name "GK selection effect". (Because of their large Balmer jumps and their higher luminosities, A stars paired with sd's would

[1]We will use the term "G/K" to include late–F stars as well as G and K stars. We will use the term "A/F" to refer to A and early–F stars.

[2]Note that despite the name, subdwarf O/B stars are not necessarily from Pop II. They merely appear below the main sequence in a color–magnitude diagram.

not likely have been selected in the initial PG survey for $U - B$ excess. On the other hand, an atypically low–luminosity sd star, paired with a MS G or K companion, might also have a detectable K–line in the PG survey spectra. As noted above, G/K companions are indeed found for many of the PG hot sd stars, based on NIR colors; thus, many sd+G/K systems are *not* subject to the "GK selection effect", and the term is to some degree a misnomer.)

It is desirable to have a catalog of hot subdwarf stars that is truly representative of the space distribution of these objects. While the PG catalog, by its design, would not be sensitive to sd+A systems, the question has lingered among hot subdwarf aficionados whether it is less complete than it could be with respect to sd+MS binaries where the MS star is of type F–G–K. Some brief quotations from recent conference papers illustrate the concern: (1) "The PG survey is biased against companions of G and K spectral type as any target with a spectrum showing Ca II H–lines [sic] was taken off the survey. This should be taken into account when looking at the companions of sdBs as most of the ones from the PG survey will be WDs [white dwarfs] instead of main sequence stars. This has important consequences when one intends to compare binary formation models with observations. It is difficult to assess how important this bias is." (Morales-Rueda et al. 2004); (2) "The PG catalogue is biased against targets that show a Ca II H–line [sic] (as these were taken out of the catalogue), and thus, against sdB binaries with main sequence companions." (Morales-Rueda et al. 2005); and (3) "to avoid the uncertain biases of the Palomar Green and other surveys..." (Morales-Rueda et al. 2006).

There are 1125 K–line stars rejected from the PG catalog, but retained in an unpublished list. If many or most of these are in fact found to be sd+MS binaries rather than sdF interlopers as Green et al. (1986) supposed, and they turn out to have short orbital periods, the Han et al. (2003) evolution scenario (which predicts them) may be strengthened and a missing class of sdBs found; at the same time there would be a large increase in the total numbers of sd stars from the PG survey. There would be important implications for the origins and also the space density, progenitors, and formation rates of such objects. If, however, the list of rejected PG candidates does not contain a large fraction of composite sd+MS binaries, it is still important to know what kinds of objects were excluded in the spectroscopic filtering of PG candidates, so that model sd populations can be "observed" in the same way that the PG catalog was constructed. Which is the actual situation?

Optical studies (broad–band photometry, moderate resolution spectroscopy) cannot easily distinguish an sdF star from a sdB+F composite. Metal–poor sdF stars lie above the Population I main sequence in the $U - B$, $B - V$ two–color diagram, owing to reduced line blocking, and thus may possibly be confused with composite sd+F systems, where the UV excess comes from the sd's contribution. Likewise, an sd star would dilute the metal lines

in a Population I F star's spectrum while maintaining the strength of the hydrogen lines (since these appear in both spectra). Similar arguments apply to the confusion between sdG and sd+G/K systems, if the sd star has a lower luminosity; such low luminosity hot subdwarfs are predicted by Han et al. (2002, 2003) to come about via evolution from intermediate mass stars which undergo RLOF mass loss. In the far UV, however, the distinction between sdF/sdG stars and sdB+MS composites is easy to make. With its UV sensitivity, positional accuracy and precision, and wide sky coverage, the GALEX satellite provides an opportunity to determine the nature of the stars rejected from the PG survey.

We note that the combination of far UV photometry from space with ground–based work has led in the past to the identification of sd+MS systems. An early example is the case of HD 17576, studied with the S2/68 experiment about the TD–1 satellite (Darius & Whitelock 1978; Olsen 1980). Although this system is actually a visual binary with an angular separation of $1\farcs8$, the photometry was of the blended sdO+G pair. Another example is that of HD 15351, a sd+F5V system (Darius 1984). Had these been fainter systems, they might have been selected as candidates in the PG survey, then rejected owing to the presence of a K–line in the optical spectrum.

To summarize, the leading scenario for the formation of sdB stars predicts that many sd+MS systems should exist, constituting a large fraction of all hot subdwarfs, but sd+A/F systems are hard to identify from optical studies. The K–line stars rejected from the PG survey are the obvious and first place to look for some of these objects. A study using GALEX photometry for a subset of the PG rejects, combined with existing visible and NIR information on these stars, allows a clear sorting into mutually exclusive categories of metal–poor sdF/G stars and the more interesting sd+MS cases. If these objects are in fact sd+MS binaries, they will be strongly detected in both the near–ultraviolet (NUV) and far–ultraviolet (FUV) GALEX passbands. If they are actually sdF/G stars, as originally supposed by the compilers of the PG catalog, then they will be readily detected in the GALEX NUV band but *not* in the FUV band. Such a study addresses the origin of hot subdwarf stars very directly. Further, if the yield of sd+MS binaries from these rejected PG candidates is high, it may help to create an enlarged and more representative catalog of such objects.

In this paper, we present a first assessment of the sd+MS binary content among the PG–rejected stars. In §2 we present the far UV, visible, and NIR photometry for a sample of 88 objects. We also present results for a small number of known hot subdwarfs and other stars, and for field F stars, to facilitate interpretation of the results in terms of modeled colors. We interpret the results in §3, where we discuss five individual objects that can be interpreted as composite hot+cool objects, but only three of which are likely consistent

with being sd+MS binaries. We also discuss the implications for the entire group of 1125 PG–rejected stars as a whole, and we point out the desirability of an enlarged study, both to increase confidence in this preliminary results and to identify individual sd+MS or other composite objects for follow–up study. We summarize our findings in §4.

2. PHOTOMETRY OF PG–REJECTS

The essential idea underlying this study is to test, for each "PG–Reject" (PGR) object, whether the UV energy distribution indicates the presence of a hot stellar source accompanying the star that is responsible for the K line or the G band. If no hot subdwarf is present, the far UV flux will fall steeply toward shorter wavelength, and an ultraviolet–based color will be very "red". In this case the favored interpretation is that the PGR is a single, late–type MS star, possibly metal–poor owing to its method of selection. (We use solar–metallicity stars to model the composite systems, since we expect the supposed hot subdwarf in such a system to have formed from an intermediate mass star.) We use the GALEX archive to collect the UV flux information. The GALEX spacecraft is currently performing a number of imaging surveys over most of the sky, using a far–ultraviolet "FUV" band (1350–1750 Å) and a near–ultraviolet "NUV" band (1750–2750 Å). See Martin et al. (2005) for a general description of GALEX and Morrissey et al. (2007) for details of the instrument calibration and data products. We also make use of NIR photometry to aid in classifying the cool stars in these systems (§2.3).

We use F and N in formulas as symbols for the AB magnitudes measured in the FUV and NUV bands, respectively. The $F-N$ color is the main quantity of interest, but interpretation is enhanced with the addition of the $N-V$ color, where V is from the Johnson UBV system. We employ synthetic photometry as a guide to the expected colors of single or blended objects.

From the 1125 PGRs, we selected 88 as the subject of this first assessment using GALEX. These 88 are the majority of the PGRs for which GALEX photometry was available in data release GR1. Table 1 presents the names of these objects along with the names of their 2MASS (Skrutskie et al. 2006) counterparts. The IAU–registered names are of the form `PGR JHHMMm+DDMM`, where minutes of Right Ascension (RA) are truncated after the first decimal. The designation style is distinct from that used for PG objects, and is sufficiently detailed to give a unique name to each PGR object. These names are based on the coordinates of the objects as recovered from the USNO–A2 catalog (Monet et al. 1998), which is based on the Palomar Observatory Sky Survey (POSS) plates taken in the 1950s. (The original finding charts for the PGRs are enlarged prints from the POSS.) The 2MASS names are

also in equatorial coordinate form, based on observations at a much more recent epoch. The 2MASS names suffice to allow precise and unambiguous identification of the star, thus we do not provide separate columns with RA and Declination.

2.1. GALEX Photometry

Ultraviolet photometry of the PGRs as obtained by GALEX is presented in Table 2, along with an estimate of the V magnitude (see §2.2), color excess E($B-V$), and colors derived from the photometry. GALEX Release 2/3 was most recently interrogated in May 2008, using the Cross–Correlation search page of the Multimission Archive at Space Telescope (MAST)[3]. The search radius used was 6 arcsec.

Table 2 lists F and its error in the AB system (Morrissey et al. 2007) or an upper limit on F. It also lists N and its error. All the PGRs discussed here were detected by GALEX in the NUV band. Sixteen were also detected in the FUV band. In the case of multiple observations of a source by GALEX, we merged the data into single best estimates of F and N using weighted averages. The quoted errors refer to these best estimates. Magnitudes and colors are rounded to two decimal places, with a floor of 0.01 mag placed under the magnitude errors. When a source was not detected in the FUV band, we calculated the flux upper limit as three times `fuv_ncat_fluxerr`, which is the tabulated error in the net FUV flux, measured at the position of the NUV detection. This flux limit is translated to AB magnitude units; the $\sigma(F)$ error column in Table 2 is left blank for upper limits.

Of the sixteen FUV detections, twelve were from short GALEX observations that were part of the All–sky Imaging Survey (AIS), one was from a longer Medium Imaging Survey (MIS) observation, two were from longer Guest Investigator (GI) observations, and one was from a very long observation in the direction of the Lockman hole (LOCK). FUV–band non–detections of the other 72 PGRs were generally for sources only observed in AIS fields, but in a few cases MIS, GI, LOCK, or Nearby Galaxy Atlas (NGA) observations were able to set more stringent upper limits on the FUV flux. Remarks in Table 2 indicate whether observations other than AIS were available.

[3] `http://archive.stsci.edu/index.html`

2.2. Visual Photometry

Estimates of V are generally only photographic, since the PGRs are generally too faint to have been the subject of individual photoelectric photometry and too bright to be observed without saturation by the Sloan Digital Sky Survey (SDSS) in the area of overlap. For the photographic V estimates, we used the prescription from Salim & Gould (2003) to convert from the USNO–A2 red and blue magnitudes:

$$V = R_{\rm USNO} + 0.32(B_{\rm USNO} - R_{\rm USNO}) + 0.23$$

These are indicated in Table 2 by the symbol "A" in the "Ref" column. The symbol "B" in this column indicates that V is estimated from SDSS g and r magnitudes according to the prescription of Jester et al. (2005):

$$V = g - 0.58(g - r) - 0.01$$

We only used SDSS data that were unsaturated in both g and r. Symbol "C" indicates photoelectric UBV photometry carried out by R.F.G. during the original PG survey. Symbol "D" indicates photoelectric CCD photometry in V and I by the All Sky Automated Survey[4] (ASAS: Pojmanski 2002). In total, 24 PGRs in Table 2 have photoelectric photometry. The tabulated V magnitudes are rounded to 0.1 mag. Based on the references cited or our own investigations, the uncertainties in the transformed or measured V magnitudes are $\sigma(V) \approx 0.03$ for objects observed photoelectrically by SDSS; $\sigma(V) \approx 0.07$ mag for R.F.G.; and $\sigma(V) \approx 0.05$ for ASAS. Photographic estimates have $\sigma(V) \approx 0.25$ mag.

Colors $F - N$ and $N - V$ are given in Table 2, along with a dereddened color $(N - V)_0$, where we have taken the color excess to be

$$E(N - V) = 4.8E(B - V)$$

as suggested by the GALEX exposure time calculator for a flat–spectrum source ($f_\nu = \text{const}$) and assuming that $A(V) = 3.2E(B - V)$. The interstellar reddening of $F - N$ is small, $E(F-N) \approx -0.1E(B-V)$, and this correction has been neglected. The tabulated $E(B-V)$ estimates are those returned from the MAST query, based on the Schlegel et al. (1998) reddening maps. They represent the full galactic extinction along the line of sight and should be appropriate for these PGR objects, which are generally expected to lie well above the Galactic plane. Color errors can be estimated by combining in quadrature the errors of the individual bands.

[4] `http://www.astrouw.edu.pl/asas/`

The V magnitude range is 11.2 to 16.3 (median near 14.7, although for PGRs with detected flux in the FUV band the median V is 13.3). The range of N magnitudes is 13.7 to 20.4. *Detected* F magnitudes range from 13.5 to 24.3; *upper limits* on F range from 21.1 to 23.5. Color excess $E(B-V)$ from Schlegel et al. (1998) ranges from 0.008 to 0.264 mag.

Figure 1 presents a $(F-N)$, $(N-V)_0$ two–color plot of the observations. Solid lines show model loci for solar and metal–poor synthetic spectra at $\log g = 5.0$ (Kurucz 1998), convolved with the GALEX FUV and NUV bandpasses and an approximate Johnson V bandpass. The GALEX post–launch response curves were obtained from the GALEX Guest Investigator website. The V bandpass was approximated as having a square response over 5150–5950 Å. The metal–poor locus is truncated at 8000 K, somewhat hotter than the Pop II turnoff. Dotted lines show the colors of composite models, combining a sd and a cool MS star to make a sd+MS system. For these loci, the subdwarfs are represented by models having [Fe/H] = 0.0, $\log g = 5.0$. These models are assigned $M_V = 3.59, 4.05$, and 4.60 for $T_{\rm eff} = 25000, 30000$, or 35000 K, respectively, derived from the luminosities of zero–age extended horizontal branch (ZAEHB) models of Caloi (1972) using suitable bolometric corrections. Each ZAEHB model generates one of the three loci shown, as it is combined with light from the companion MS star. The MS stars are represented by models having [Fe/H] = 0.0, $\log g = 5.0$ and $T_{\rm eff}$ ranging from 4000 K to 9750 K. Absolute V magnitudes of the cool models are adopted MS values. The loci of composite models "loop back" to the left in the Figure, as the MS component's $N-V$ color index decreases with increasing $T_{\rm eff}$ at the same time that the MS component begins to dominate the combined light of the sd+MS system. For the adopted ZAEHB absolute magnitudes, this happens when the MS star has an F spectral type.

Open circles in Figure 1 show the colors of six stars classified by Green et al. (1986) as hot subdwarf stars (Table 3). Estimated reddening is again from Schlegel et al. (1998) via MAST; here we have dereddened both $F-N$ and $N-V$ to facilitate comparison with the model loci. Note, however, that non–linearity of the GALEX photometry at these magnitudes may be important (Morrissey et al. 2007). From 2MASS photometry (see, e.g., Stark & Wade 2003), PG 0105+276 and TON 349 are regarded as photometrically "composite" while the remaining stars are regarded as single. Note that PG 0105+276 is a close visual pair with separation $\approx 4''$; we treat the F, N, and V measurements for this object as referring to the combined light from this pair.

2.3. Near–Infrared Photometry

NIR colors from 2MASS for all of the PGR stars in this study are shown in panel (a) of Figure 2. The MS locus of Bessell & Brett (1988) is also shown, converted to 2MASS colors using the prescription of Carpenter (2001). Panel (b) of Figure 2 shows the NIR colors of stars selected from the abundance compilation of Cayrel de Strobel et al. (2001), with $V > 8.5$, $T_{\rm eff} > 5000$ K, $\log g > 3.5$, and $E(B-V) < 0.20$. We retained 27 Cayrel stars with [Fe/H] between -0.3 and $+0.3$ ("solar") and 27 stars with [Fe/H] between -1.8 and -1.2 ("metal–poor"). These two groups are indistinguishable by location in the NIR two–color diagram; moreover, the NIR colors of PGR objects closely follow the same locus within the errors of measurement.

3. DISCUSSION

3.1. Overview

Inspection of Fig. 1 shows that among the PGRs with detections in the FUV band, three lie near the hot end of the stellar locus ("hot" is noted in the Remarks column of Table 2 for these). Eleven lie near the loci shown for single stars at $T_{\rm eff} \sim 7000$ K, and two lie above and to the right of this position ("comp?" in Table 2). We summarize the GALEX, visual and NIR photometry for the five "hot" or "comp?" stars in Table 4. All of the upper limits on F result in placement of PGRs well away from the part of the diagram that characterizes blended light from a sd+MS system. This is the main result of our study: *most of the PGRs in this sample are not binary systems containing a hot subdwarf star and a MS star.*

3.2. Validity of GALEX Photometry

The three "hot" PGRs all have F and N magnitudes brighter than 15.4. The measured count rates in the GALEX detectors for these brightness levels may be subject to non–linearities and other "saturation" or "fatigue" effects, characterized *statistically* by "roll–off curves" (see Morrissey et al. 2007, Fig. 8). For the brightest of the three "hot" PGRs, PGR J00075+0542, MAST returned two distinct entries, with F differing by 1.0 mag and N differing by 0.3 mag in the opposite sense. Clearly, the vertical position of this object in Fig. 1 is uncertain by $\sim$0.5 mag, much larger than the formal error bars reported by MAST and tabulated here. Fortunately for this study, even an error of 0.5 mag in $F-N$ does not vitiate the conclusion as to the nature of this object, which clearly contains a hot star. (As

we did for all other stars with multiple observations, we have averaged the magnitudes for PGR J00075+0542.)

Some of the scatter in $F-N$ (and $N-V$) for the known hot subdwarfs of Table 3 may also be due to the "non–linearity" and other performance issues in GALEX photometry of bright point sources, as discussed above. In this paper, we take the reported photometry and errors at face value for discussion purposes, since it does not affect the bulk of our sample. Detailed modeling of bright composite objects should not rely too heavily on GALEX photometry, however.

3.3. Validity of Model Loci

Despite the uncertainty in positioning the known hot subdwarfs in Fig. 1, it is evident that the synthetic photometry is in reasonable agreement with the observations of these hot stars. PG 0105+276 has been classified as sdO(B) and sdB+K7 (visual double). PG 0212+148 has $T_{\rm eff}$ near 25000 K. PG 2356+167 is classified sdB-O by Green et al. (1986) but "non–sd" by Saffer (1991) who notes the Ca II K line in the spectrum; Saffer et al. (1997) estimate $T_{\rm eff} = 23800$ K, $\log g = 4.70$, while Lynn et al. (2004) classify this object as B2V (evolved) and estimate $T_{\rm eff} \approx 20000$ K and $\log g = 4.3$. The remaining stars are classified "sdO(B)" or "sdB" by Green et al. (1986).

To see how well the model loci of cooler single atmospheres match the GALEX observations, we collected photometry for a sample of 30 lightly–reddened F star candidates ($E(B-V) < 0.04$), selected on the basis of their 2MASS colors. The intrinsic 2MASS colors of F0–F7 dwarfs were determined from stars classified on the MK system by Houk & Swift (1999). V magnitudes for the sample discussed here were collected from ASAS and range between 11.2 and 12.5. The GALEX N magnitudes range from 14.6 to 17.0 with nominal errors $\sigma(N) < 0.03$, while F ranges from 18.9 to 23.2 with median error $\sigma(F) = 0.23$ (maximum $\sigma(F) = 0.52$). These stars are displayed in the $(F-N)$, $(N-V)_0$ two–color diagram in Figure 3, where typical 1σ error bars are the size of the plotting symbol or smaller. The model loci for single stars from Figure 1 are supplemented with additional loci.

The observed candidate F stars generally lie near the [Fe/H] = 0.0 loci as expected, but there is some scatter to "bluer" $F-N$ values, somewhat larger than might be expected from the typical error of measurement. (The range of $T_{\rm eff}$ inferred from the $(N-V)_0$ colors of these stars is in good accord with that of F2–F7 dwarfs of Population I, as suggested by the 2MASS photometry. Thus, the scatter does not seem attributable to $(N-V)_0$.) A tentative interpretation is that the upward scatter may be caused by unmodeled chromospheric or

transition region activity which varies in strength from star to star. This might be manifested, for example, by emission at the C IV 1548, 1550 Å doublet, which is located near the peak of the GALEX FUV passband. With this caveat, we conclude that the single star synthetic photometry based on Kurucz (1998) models provides an acceptable basis for constructing colors of composite models and for interpreting the photometry of PGR objects.

3.4. Interpretation of the Two–Color Diagrams

Stark & Wade (2003) showed that hot subdwarf stars with $J - K_s \gtrsim +0.15$ form a distinct group which can be modeled as photometrically composite, with the cool companion star consistent with a dwarf of spectral type (SpT) F, G, or K. This result is confirmed by spectra of a subset of such systems (Stark 2005; Stark & Wade 2006). Of course, late–type stars that are single also have red $J - K_s$ colors, thus 2MASS data alone do not suffice to indicate whether a red object is a composite system with a hot subdwarf and a cool star. It is the combination of GALEX and 2MASS data that allows a composite system to be recognized.

Based on the GALEX photometry shown in Figure 1, there is a hot star present in each of the three PGRs labeled "hot" in Table 4. Considering also their NIR and $V - K_s$ colors, they are all photometrically composite. If PGR J00075+0542 were a single star, its NIR colors would indicate a SpT near F2, but the cool star may be slightly later than this, given the dilution by the hot component. Dilution should be more evident in the $V - K_s$ color index, and indeed it suggests a SpT near F0 under a single–star interpretation. By the same reasoning PGR J22451+2134 contains a cool star with SpT somewhat later than K0. PGR J23025+2602's cool component must have SpT later than about F8. The GALEX photometry supports this ordering by color (given the uncertainty in the measured N magnitudes). In particular, PGR J00075+0542 has the earliest cool component based on visual and NIR colors, and has the *reddest* $(N - V)_0$ color among the three "hot" PGRs, a result entirely consistent with combining some hot ZAEHB subdwarf with MS companions of different temperatures and luminosities in the three cases.

Schuster et al. (2004) independently studied PGR J00075+0542, their name for this object being BPS CS 31070–0080. They classified it as a "sub–luminous blue horizontal branch star" (SL–BHB).

The $(N - V)_0$ indices are consistent with roughly equal absolute V magnitudes of the hot and cool components in each system. The interpretation that these three PGRs are sd+MS systems is perhaps not unique; however, the spectroscopic type of "sdG" assigned by

Green et al. (1986) in each case supports the argument that the cool components are dwarfs rather than evolved stars. Pending further study to establish more accurate temperatures, gravities, and metallicities, we adopt the sd+MS picture as the best interpretation of the data.

Based on GALEX and V data alone, the two "comp?" stars in Table 4 might simply be F or G dwarfs with high activity levels: they lie within the extreme limits of the scattering of candidate F stars in Figure 3. On the other hand, a composite system is not ruled out in either case, although it would not be consistent with a MS star paired with a ZAEHB star. The NIR colors for PGR J08401+4421 correspond to a (single) dwarf of SpT near G0, while $V - K_s$ suggests the SpT is near G5 and $(N - V)_0$ suggests $T_{\rm eff} \approx 6800$ K. These are slightly inconsistent with the expectation for a hot+cool binary, in terms of the ordering of implied temperature by wavelength. Nevertheless, we conducted numerical experiments, adding a hot component to a Kurucz model with $T_{\rm eff} \approx 6800$ K. The results suggest that such a hot component would need to be about 4 mag fainter than the cool star at V, in order to reproduce the GALEX colors. In such a case, the hot star would be fainter than a typical hot subdwarf, or the cool star would need to be brighter than a MS star. A white dwarf is a possible hot component, although $T_{\rm eff} \gtrsim 30000$ K is required if its radius is that of a $\sim 0.6\,M_\odot$ remnant. The cooling time of such hot white dwarfs is short (Wood & Winget 1989). A similar analysis applies for PGR J02040+1500, whose NIR and $V - K_s$ colors suggest a SpT near G5 or G8, but whose $(N - V)_0$ index suggests a warmer star with $T_{\rm eff} \approx 6500$ K (using the solar metallicity loci). The $F - N$ and $(N - V)_0$ colors can be roughly matched by combining a $T_{\rm eff} \sim 6500$ K star and a hot star that is $\sim$4 mag fainter at V. Improved visual photometry of these systems and accurate luminosity (and metallicity) classifications of their cool stars would help clarify the nature of the hot component.

The remaining eleven PGR objects that were detected in the FUV band lie close to the low–metallicity (Pop II) MS locus in Figure 1, although with some scatter. This is consistent with the spectroscopic classification of "sdG" (with slight variants) given to these objects in the original PG survey. No indication of the presence of a hot stellar component is given by the GALEX photometry of these stars. The 72 upper limits for other PGRs shown in the Figure are sufficiently far removed from the locus of composite sd+MS loci that they likewise support the original sdG classifications of these objects as single stars. The NIR colors of the ensemble are consistent with a single–star interpretation, although it should be noted that the (Population I) SpTs indicated extend to K0 ($T_{\rm eff} \approx 5200$ K), whereas the $(N - V)_0$ data suggest a lower bound of $T_{\rm eff} \gtrsim 5700$ K (solar metallicity) or $T_{\rm eff} \gtrsim 5200$ K (metal–poor).

Three stars, PGR J09281+6503, PGR J09395+6353, and PGR J10273+5758, for which

UBV data are available, lie slightly above the Hyades main sequence in the $(U-B)$, $(B-V)$ two–color diagram with $B-V$ in the range +0.50 to +0.63 and $U-B$ in the range −0.124 to +0.07, just where reduced metal line blanketing would place a sdG star. The first of these stars was detected in the FUV band and lies very near the low–metallicity locus in Figure 1, near $T_{\rm eff} = 6000$ K.

The occasional large offsets between USNO–A2 and 2MASS catalog positions, noted in Table 1, suggest that a few stars of high proper motion may be included in this sample of PGR objects. This view is confirmed by proper motion data for 61 stars of the sample, obtained from the Second U.S. Naval Observatory CCD Astrograph Catalog (UCAC2: Zacharias et al. 2004). Stars with large Table 1 offsets tend to have larger than average components of proper motion to the West, with amplitudes $\mu_\alpha \sim -25\,{\rm mas\ yr}^{-1}$ (corresponding to transverse velocities $v_T \sim 100\,{\rm km}^{-1}$ for distances $d \sim 1000$ pc). The direction of motion is opposite to that of the Local Standard of Rest, and thus an interpretation in terms of thick disk or galactic halo rotation for this group of stars is tempting, although only weakly indicated.

3.5. Implications for the PGRs as a Class

The PG catalog is the single largest contributor to the list of spectroscopically identified hot subdwarf stars (Kilkenny et al. 1988). Because it has reasonably well–defined magnitude and color limits, it is often used as the source of moderately bright sdB/sdO stars on which to do time–series photometry, radial velocity orbital studies, etc. It also has been used for comparison against population synthesis models in studies of the origin of hot subdwarfs. Every catalog that strives to be complete will suffer from two types of error, that of including objects that do not belong, and that of excluding objects that do belong. Concerns have been raised about the hot subdwarf part of the PG catalog, in regard to this second type of error. For this reason we looked again at a sample of the stars rejected from the PG catalog.

Only three of the 88 PGR objects examined in this paper show a photometrically composite character, consistent with a sd+MS system. Two additional objects *may* be photometrically composite, although in these cases the data do not support a sd+MS interpretation. The great majority of the PGR stars appear to be consistent with single stars on the lower MS, perhaps chromospherically active, perhaps metal poor. Additional data, such as UBV colors for a few stars, support a metal–poor classification in those cases. As originally explained by Green et al. (1986), the PG survey photographic photometry was imprecise enough to allow the selection of numerous *candidate* UV–excess stars which were in fact not "hot" in the desired sense of meeting a color threshold of $U-B < -0.46$. The survey spectroscopy was used to weed these out, leaving only "hot" objects in the final PG

catalog. That the rejected candidates (PGRs) are almost entirely metal–weak sdF or sdG stars is entirely consistent with the nature of the PG survey; this is because the most likely contaminant, based on a measured $U-B$ color accidentally crossing the color threshold for the survey, would be an F or G star with reduced metal line blanketing. That a few systems were rejected which do in fact contain a hot star (likely a subdwarf B or subdwarf O star) should not be especially surprising, if they were paired with cooler stars, depending on which star dominates the photographic region of each blended spectrum.

This paper exploits the wider wavelength range enabled by the GALEX and 2MASS projects to further characterize these systems. The quantitative result is that the fraction of such hot+cool systems among the PGR objects that comprise the present sample is small. An important question is whether this conclusion extends to the entire list of 1125 PGRs. The PGR list is not uniform with respect to $U-B$, nor with respect to limiting B magnitude. This is because in some PG survey fields, classification spectroscopy was started before a final $U-B$ color (transformed from photographic magnitudes) was available. Thus some UV–excess *candidates* were rejected that were ultimately measured to be redder than the color cutoff of the PG survey. The present sample was drawn from a subset of PG survey fields that were observed early in the GALEX observational program, and it may draw more or less heavily from PG fields with an "extra" supply of PGRs. A wider study of the PGR list is therefore needed to confirm whether the present result, a $\sim 3/88$ rate of incidence of sd+MS systems, is representative of the PGR stars overall. Because of the non–uniformity of the PGR list, this would be not merely a refinement in the statistical precision of the present result, but a necessary confirmation or improvement. An additional benefit of a significantly larger sample would be to more firmly establish the ratio of F–type companions to G– or K–type companions in the sd+MS systems that are found. In the Han et al. (2002, 2003) binary population synthesis models, this ratio is strongly related to the critical mass–ratio parameter, which serves to separate stable and unstable mass transfer cases. Finally, it is important to identify those individual PGR stars from the entire list that *are* photometrically composite, for appropriate follow–up studies, including the measurement of orbital periods.

We can attempt a cautious extrapolation of the results of the present sample of 88 stars to the full 1125 PGR objects. At present, there is no evidence to suggest that the present sample of 88 differs systematically from the full sample, so such extrapolation may be a useful guide to what may be expected, bearing in mind the caveats stated above. Taking 3/88 as the rate of incidence of sd+MS systems in the full sample, we predict ∼38 "new" sd systems will be found among the PGR stars. This is to be compared with the ∼40% of sdB stars in the Kilkenny et al. (1988) catalogue that were found by Stark et al. (2004) to have a cool companion; applied to the ∼900 PG stars in Kilkenny et al. (1988), this amounts to ∼360 sd+MS stars. The "new" sd+MS systems that might result from a study of the

full PGR list thus represent a ∼10% increase in this roughly magnitude-limited sample. We would not be surprised to find that the rate of incidence of sd+MS systems in the full PGR list may be ∼ 2× smaller or larger than 3/88 (3.5%), either from small-number statistics or "bad luck" in drawing our small sample from a few fields. Thus the addition of new hot sd+MS systems from among the PGR objects to those found in the PG catalog may plausibly be expected to be at the 5–20% level, a consequence of the large numbers of PGR objects, coupled with a fairly small rate of incidence of sd+MS binaries in the PGR list.

4. SUMMARY

We have presented UV, visual, and NIR photometry of a sample of candidate objects rejected from the final PG catalog. We analyzed the photometry in color–color diagrams, aided by synthetic photometry of single and binary stars and by empirically determined colors of stars of various types. Sixteen of the 88 PGRs were detected in both the FUV and NUV channels of GALEX imaging. Of these, eleven are consistent with being single cool stars, as are the 72 cases where only an upper limit on the FUV flux was obtained. Thus, most of these PGRs have colors that are consistent with those of single cool stars, possibly metal–poor. This is consistent with the removal of these candidate UVX stars from the PG survey, based on spectroscopy. Of the remaining five stars, three exhibit composite colors consistent with a sd+MS interpretation, and the other two may be single or composite.

The GALEX AIS survey is sufficient to detect a hot component in a PGR, if one is present. Thus it should be possible to extend the present study of 88 PGRs to include most of the 1125 objects in the full list, which is desirable given the non–uniform nature of the PGR list. Such an extension would establish definitively whether the PGR list does or does not harbor a large number of sd+MS binaries or other hot+cool systems, putting to rest the concern about the completeness of the PG catalog (within its declared magnitude and color limits) with regard to hot subdwarfs, hot white dwarfs, etc. It would provide a more robust measurement of the frequency of occurrence of early–F companions, compared with late–F/G/K companions. Finally, it would identify those individual PGRs that are photometrically composite, to allow appropriate follow–up studies. We are currently undertaking this larger study.

We thank David Monet for providing a copy of the USNO–A2 catalog, and John Feldmeier and Bruce Koehn for assistance in the installation and use of the software package Refnet, which we used to access the catalog. We also thank Luciana Bianchi for helpful correspondence regarding synthetic GALEX photometry. We thank the referee for helpful

and constructive comments. Support from NASA grants NGT5–50399, NNG05GE11G, and NNX09AC83G is gratefully acknowledged. Based on observations made with the NASA Galaxy Evolution Explorer. GALEX is operated for NASA by the California Institute of Technology under NASA contract NAS5-98034. This publication makes use of data products from the Two Micron All Sky Survey, which is a joint project of the University of Massachusetts and the Infrared Processing and Analysis Center/California Institute of Technology, funded by the National Aeronautics and Space Administration and the National Science Foundation. Some of the data presented in this paper were obtained from the Multimission Archive at the Space Telescope Science Institute (MAST). STScI is operated by the Association of Universities for Research in Astronomy, Inc., under NASA contract NAS5–26555. Support for MAST for non–HST data is provided by the NASA Office of Space Science via grant NAG5–7584 and by other grants and contracts. This research has made use of the SIMBAD database, operated at CDS, Strasbourg, France.

Facility: GALEX

REFERENCES

Allard, F., Wesemael, F., Fontaine, G., Bergeron, P., & Lamontagne, R. 1994, AJ, 107, 1565

Bessell, M. S. & Brett, J. M. 1988, PASP, 100, 1134

Brown, T. M., Bowers, C. W., Kimble, R. A., Sweigart, A. V., & Ferguson, H. C. 2000, ApJ, 532, 308

Caloi, V. 1972, A&A, 20, 357

Carpenter, J. M. 2001, AJ, 121, 2851

Cayrel de Strobel, G., Soubiran, C., & Ralite, N. 2001, A&A, 373, 159

Darius, J. 1984, Ap&SS, 99, 273

Darius, J. & Whitelock, P. A. 1978, Nature, 275, 428

D'Cruz, N. L., Dorman, B., Rood, R. T., & O'Connell, R. W. 1996, ApJ, 466, 359

Green, R. F., Schmidt, M., & Liebert, J. 1986, ApJS, 61, 305

Han, Z., Podsiadlowski, P., & Lynas-Gray, A. E. 2007, MNRAS, 380, 1098

Han, Z., Podsiadlowski, P., Maxted, P. F. L., & Marsh, T. R. 2003, MNRAS, 341, 669

Han, Z., Podsiadlowski, P., Maxted, P. F. L., Marsh, T. R., & Ivanova, N. 2002, MNRAS, 336, 449

Houk, N. & Swift, C. 1999, Michigan catalogue of two-dimensional spectral types for the HD Stars ; vol. 5 (Ann Arbor, Michigan : Department of Astronomy, University of Michigan.)

Jester, S., Schneider, D. P., Richards, G. T., Green, R. F., Schmidt, M., Hall, P. B., Strauss, M. A., Vanden Berk, D. E., Stoughton, C., Gunn, J. E., Brinkmann, J., Kent, S. M., Smith, J. A., Tucker, D. L., & Yanny, B. 2005, AJ, 130, 873

Kilkenny, D., Heber, U., & Drilling, J. S. 1988, South African Astronomical Observatory Circular, 12, 1

Kurucz, R. 1998, *Solar abundance model atmospheres for 0,1,2,4,8 km/s.* (Cambridge, Mass.: Smithsonian Astrophysical Observatory), http://kurucz.harvard.edu/

Lisker, T., Heber, U., Napiwotzki, R., Christlieb, N., Han, Z., Homeier, D., & Reimers, D. 2005, A&A, 430, 223

Lynn, B. B., Keenan, F. P., Dufton, P. L., Saffer, R. A., Rolleston, W. R. J., & Smoker, J. V. 2004, MNRAS, 349, 821

Martin, D. C., Fanson, J., Schiminovich, D., Morrissey, P., Friedman, P. G., Barlow, T. A., Conrow, T., Grange, R., Jelinsky, P. N., Milliard, B., Siegmund, O. H. W., Bianchi, L., Byun, Y.-I., Donas, J., Forster, K., Heckman, T. M., Lee, Y.-W., Madore, B. F., Malina, R. F., Neff, S. G., Rich, R. M., Small, T., Surber, F., Szalay, A. S., Welsh, B., & Wyder, T. K. 2005, ApJ, 619, L1

Mengel, J. G., Norris, J., & Gross, P. G. 1976, ApJ, 204, 488

Monet, D. B. A., Canzian, B., Dahn, C., Guetter, H., Harris, H., Henden, A., Levine, S., Luginbuhl, C., Monet, A. K. B., Rhodes, A., Riepe, B., Sell, S., Stone, R., Vrba, F., & Walker, R. 1998, The USNO-A2.0 Catalogue (U.S. Naval Observatory Flagstaff Station [USNOFS] and Universities Space Research Association stationed at USNOFS)

Morales-Rueda, L., Maxted, P. F. L., & Marsh, T. R. 2004, Ap&SS, 291, 299

Morales-Rueda, L., Maxted, P. F. L., Marsh, T. R., Kilkenny, D., & O'Donoghue, D. 2005, in ASP Conf. Ser. 334, 14th European Workshop on White Dwarfs, ed. D. Koester & S. Moehler, 333

Morales-Rueda, L., Maxted, P. F. L., Marsh, T. R., Kilkenny, D., & O'Donoghue, D. 2006, Baltic Astronomy, 15, 187

Morrissey, P., Conrow, T., Barlow, T. A., Small, T., Seibert, M., Wyder, T. K., Budavári, T., Arnouts, S., Friedman, P. G., Forster, K., Martin, D. C., Neff, S. G., Schiminovich, D., Bianchi, L., Donas, J., Heckman, T. M., Lee, Y.-W., Madore, B. F., Milliard, B., Rich, R. M., Szalay, A. S., Welsh, B. Y., & Yi, S. K. 2007, ApJS, 173, 682

O'Connell, R. W. 1999, ARA&A, 37, 603

Olsen, E. H. 1980, Information Bulletin on Variable Stars, 1770, 1

Pojmanski, G. 2002, Acta Astronomica, 52, 397

Saffer, R. A. 1991, PhD thesis, University of Arizona

Saffer, R. A., Bergeron, P., Koester, D., & Liebert, J. 1994, ApJ, 432, 351

Saffer, R. A., Keenan, F. P., Hambly, N. C., Dufton, P. L., & Liebert, J. 1997, ApJ, 491, 172

Salim, S. & Gould, A. 2003, ApJ, 582, 1011

Schlegel, D. J., Finkbeiner, D. P., & Davis, M. 1998, ApJ, 500, 525

Schuster, W. J., Beers, T. C., Michel, R., Nissen, P. E., & García, G. 2004, A&A, 422, 527

Skrutskie, M. F., Cutri, R. M., Stiening, R., Weinberg, M. D., Schneider, S., Carpenter, J. M., Beichman, C., Capps, R., Chester, T., Elias, J., Huchra, J., Liebert, J., Lonsdale, C., Monet, D. G., Price, S., Seitzer, P., Jarrett, T., Kirkpatrick, J. D., Gizis, J. E., Howard, E., Evans, T., Fowler, J., Fullmer, L., Hurt, R., Light, R., Kopan, E. L., Marsh, K. A., McCallon, H. L., Tam, R., Van Dyk, S., & Wheelock, S. 2006, AJ, 131, 1163

Stark, M. A. 2005, PhD thesis, The Pennsylvania State University

Stark, M. A. & Wade, R. A. 2003, AJ, 126, 1455

—. 2006, Baltic Astronomy, 15, 175

Stark, M. A., Wade, R. A., & Berriman, G. B. 2004, Ap&SS, 291, 333

Wesemael, F., Fontaine, G., Bergeron, P., Lamontagne, R., & Green, R. F. 1992, AJ, 104, 203

Wood, M. A. & Winget, D. E. 1989, in Lecture Notes in Physics, Berlin Springer Verlag, Vol. 328, IAU Colloq. 114: White Dwarfs, ed. G. Wegner, 282–285

Yi, S. K. 2008, in ASP Conf. Ser. 392, Hot Subdwarf Stars and Related Objects, ed. U. Heber, C. S. Jeffery, & R. Napiwotzki, Vol. 392, 3

Zacharias, N., Urban, S. E., Zacharias, M. I., Wycoff, G. L., Hall, D. M., Monet, D. G., & Rafferty, T. J. 2004, AJ, 127, 3043

This preprint was prepared with the AAS LaTeX macros v5.2.

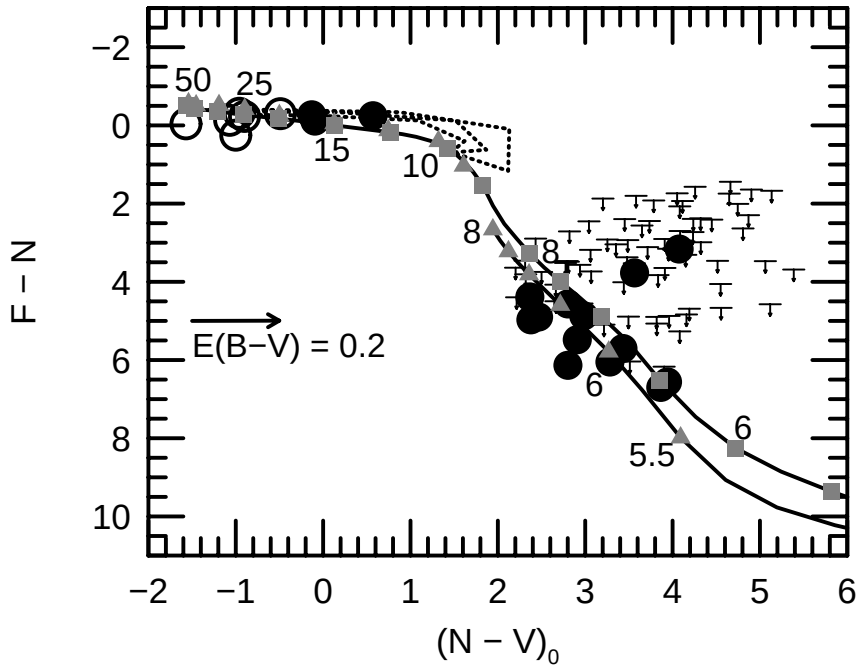

Fig. 1.— Observations of PGR objects, presented in a two–color diagram using Johnson V and GALEX F and N magnitudes. Filled circles are PGR objects detected in both F and N; horizontal bars are PGR objects detected in N but with upper limits in F (Table 2). Open circles are known hot stars (Table 3). A reddening vector for Milky Way dust is shown. Solid lines show model loci for solar and metal–poor synthetic spectra at $\log g = 5.0$ (Kurucz 1998). Grey squares ([Fe/H]= 0.0) and triangles ([Fe/H]= −1.5) along the loci are shown for $T_{\rm eff}$ = 5.5 (0.5) 8.0 (1.0) 10, 12, 15 (5) 30 (10) 50 kK, with selected points labeled. Dotted lines show colors of composite models, combining a "hot subdwarf" and a cool main sequence star (see §2.2).

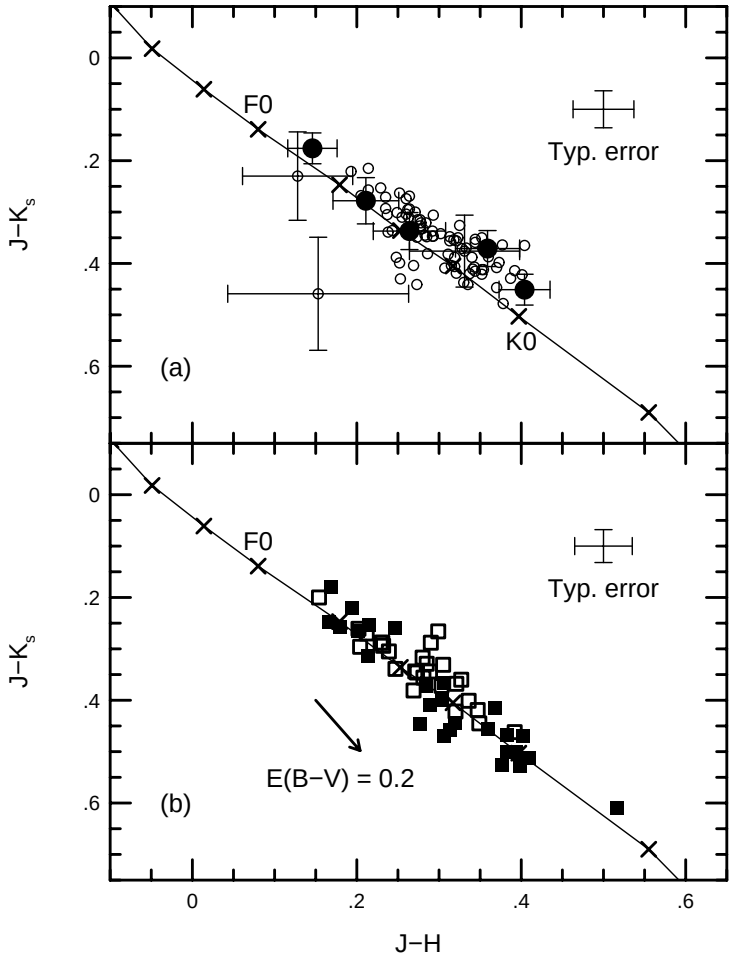

Fig. 2.— (a) NIR two–color diagram showing the PGR objects. The five "hot" or "comp?" objects of Table 4 are shown as filled circles; other PGRs are shown as small open circles. Individual error bars are shown for these five objects or in cases where $\sigma(J-H)$ or $\sigma(J-K_s)$ exceeds 0.07 mag. The median ("typical") error bar is shown in the upper right. The MS locus of Bessell & Brett (1988) is shown, converted to 2MASS colors using the prescription of Carpenter (2001); crosses indicate spectral types of A0, A5, F0, F5, G0, G6, K0, and K5. (b) The same diagram, showing the colors of the "Cayrel" sample (see §2.3). Filled squares have "solar" metallicity; open squares are "metal–poor". A reddening vector for $E(B-V) = 0.2$ is shown. No reddening correction has been applied to data in either panel.

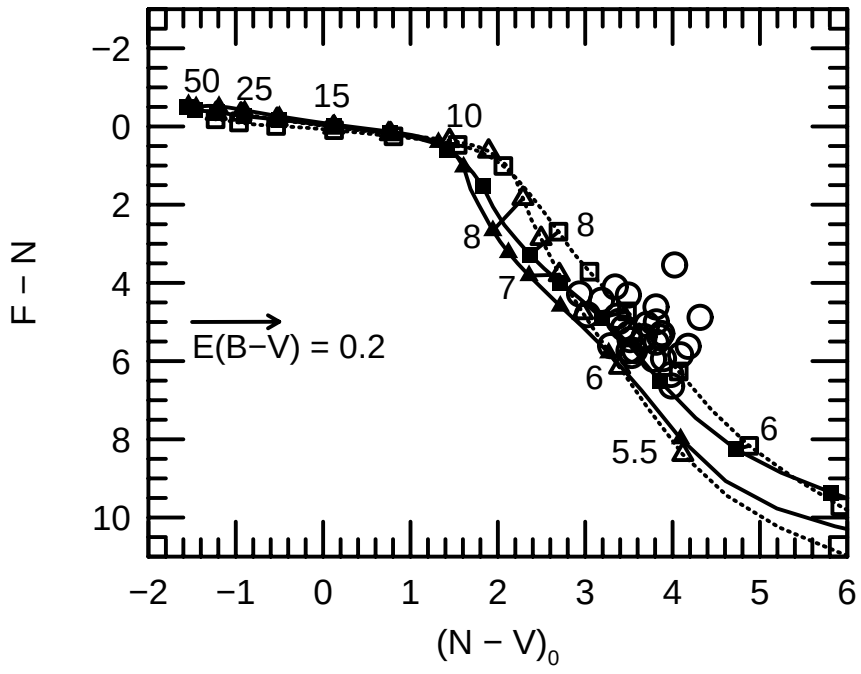

Fig. 3.— Observations of candidate F dwarfs, selected on the basis of their 2MASS colors, presented in the same two–color diagram as shown in Fig. 1. The observed $N-V$ colors have been corrected for galactic reddening. Model loci at $\log g = 5.0$ (solid lines) are shown and labeled as in Figure 1, supplemented by loci at $\log g = 3.5$ (dotted lines). All loci extend to $T_{\rm eff} = 30000$ K, with the $\log g = 5.0$ loci extending to 50000 K. Filled squares and triangles show $\log g = 5.0$ models at metallicity [Fe/H] = 0.0 and -1.5, respectively; open symbols show $\log g = 3.5$ models. "Tie–bars" connect low– and high–gravity model points for each metallicity at $T_{\rm eff} = 6000$, 7000, and 8000 K.

Table 1. PGR sources and 2MASS counterparts

PGR Name	2MASS Designation	Notes
PGR J00021+0251	2MASS J00020846+0251282	
PGR J00036+0013	2MASS J00033771+0013085	
PGR J00040+0251	2MASS J00040522+0251534	
PGR J00075+0542	2MASS J00073216+0542017	
PGR J00373+0628	2MASS J00371927+0628165	
PGR J00388+1228	2MASS J00385212+1228112	
PGR J00410+0157	2MASS J00410389+0157473	
PGR J00418+0345	2MASS J00415150+0345285	1
PGR J00434+0704	2MASS J00432693+0704389	
PGR J00446+1055	2MASS J00443778+1055320	
PGR J00451+1802	2MASS J00450738+1802573	
PGR J00515+0021	2MASS J00513429+0021393	
PGR J00547+0224	2MASS J00544424+0224060	
PGR J00550+0905	2MASS J00550423+0905570	
PGR J00577+0631	2MASS J00574772+0631090	1
PGR J00586+0431	2MASS J00583732+0431146	1
PGR J00590+1255	2MASS J00590159+1255505	
PGR J01010+2230	2MASS J01010193+2230303	
PGR J01028+1324	2MASS J01025095+1324548	1
PGR J01048+1639	2MASS J01045053+1639035	
PGR J01051+1624	2MASS J01050611+1624562	
PGR J01109+1845	2MASS J01105729+1845052	
PGR J01117+1746	2MASS J01114271+1746481	
PGR J01122+1813	2MASS J01121375+1813495	
PGR J01135+1845	2MASS J01133046+1845008	
PGR J01162+1714	2MASS J01161310+1714194	
PGR J01162+1840	2MASS J01161525+1840381	
PGR J01369+1653	2MASS J01365914+1653152	
PGR J02000+1409	2MASS J02000162+1409419	1
PGR J02040+1500	2MASS J02040015+1500434	
PGR J02047+1514	2MASS J02044221+1514550	

Table 1—Continued

PGR Name	2MASS Designation	Notes
PGR J02549+1259	2MASS J02545675+1259248	
PGR J02561+1257	2MASS J02560830+1257089	
PGR J02572+1313	2MASS J02571584+1313253	
PGR J03037+1202	2MASS J03034569+1202136	
PGR J03130+0313	2MASS J03130291+0314001	
PGR J03133+0542	2MASS J03131814+0542483	
PGR J03281+0035	2MASS J03280935+0035272	1
PGR J08237+6750	2MASS J08234774+6750216	
PGR J08315+4047	2MASS J08313260+4047091	
PGR J08391+4710	2MASS J08390680+4710519	
PGR J08392+4624	2MASS J08391477+4624416	
PGR J08401+4421	2MASS J08400897+4421272	
PGR J08430+4447	2MASS J08430003+4447280	
PGR J08430+4609	2MASS J08430306+4609075	
PGR J08431+4606	2MASS J08430627+4606269	1,2
PGR J08433+4606	2MASS J08432100+4606532	
PGR J08484+2714	2MASS J08482915+2714548	
PGR J08538+2708	2MASS J08534884+2708382	
PGR J09059+6027	2MASS J09055922+6027162	2
PGR J09069+5722	2MASS J09065794+5722567	
PGR J09087+6024	2MASS J09084225+6024023	
PGR J09165+3213	2MASS J09163419+3213061	
PGR J09190+4314	2MASS J09190162+4314000	
PGR J09233+5716	2MASS J09232048+5716029	
PGR J09281+6503	2MASS J09281137+6503311	
PGR J09322+5613	2MASS J09321441+5613272	
PGR J09343+6347	2MASS J09342377+6347564	
PGR J09370+4228	2MASS J09370212+4228321	
PGR J09395+6353	2MASS J09393451+6353016	
PGR J10170+5439	2MASS J10170106+5439076	
PGR J10173+5052	2MASS J10172228+5052286	1

Table 1—Continued

PGR Name	2MASS Designation	Notes
PGR J10203+3912	2MASS J10201970+3912284	1
PGR J10273+5758	2MASS J10272284+5758345	1
PGR J10319+6212	2MASS J10315611+6212506	
PGR J10337+5505	2MASS J10334782+5505580	
PGR J10445+5445	2MASS J10443579+5445066	
PGR J10453+5824	2MASS J10452381+5824022	
PGR J21005+0221	2MASS J21003209+0221100	1
PGR J21556+0603	2MASS J21553620+0603295	1
PGR J22172+1900	2MASS J22171637+1900375	
PGR J22199+1828	2MASS J22195611+1828022	
PGR J22216+1723	2MASS J22214179+1723557	
PGR J22247+0827	2MASS J22244501+0827532	
PGR J22263+1657	2MASS J22262100+1657432	1
PGR J22272+1721	2MASS J22271650+1721569	
PGR J22311+1648	2MASS J22311155+1648190	1
PGR J22451+2134	2MASS J22450803+2134194	
PGR J22564+2256	2MASS J22562910+2256281	1,2
PGR J22572+2215	2MASS J22571430+2215237	
PGR J23001+2512	2MASS J23000676+2512365	
PGR J23025+2602	2MASS J23023384+2602579	
PGR J23038+2731	2MASS J23034979+2731381	
PGR J23254+1236	2MASS J23252669+1236423	
PGR J23263+0259	2MASS J23262172+0259315	1
PGR J23445+0204	2MASS J23443281+0204199	1
PGR J23479+1048	2MASS J23475699+1048552	1
PGR J23562+2613	2MASS J23561539+2613419	

[1]Positional offset between USNO-A2 and 2MASS exceeds $1\farcs5$ (80th percentile of offset size).

[2]There is a second 2MASS object within 10″ of the USNO position.

Table 2. GALEX and V-band Photometry of PGR objects

Name	F (mag)	$\sigma(F)$[a] (mag)	N (mag)	$\sigma(N)$ (mag)	V (mag)	Ref[b]	$(F-N)$[a] (mag)	$(N-V)$ (mag)	E$(B-V)$[c] (mag)	$(N-V)_\circ$ (mag)	Remarks
PGR J00021+0251	21.97	···	18.14	0.04	14.2	A	$>$ 3.83	3.94	0.022	3.83	···
PGR J00036+0013	21.73	···	19.03	0.08	14.8	A	$>$ 2.70	4.23	0.030	4.09	···
PGR J00040+0251	21.75	···	18.38	0.06	14.8	A	$>$ 3.37	3.58	0.021	3.48	···
PGR J00075+0542	13.47	0.01	13.72	0.01	13.0	D	-0.25	0.72	0.031	0.57	hot
PGR J00373+0628	22.03	···	18.92	0.05	15.1	A	$>$ 3.11	3.82	0.022	3.71	···
PGR J00388+1228	21.49	···	19.69	0.11	15.7	A	$>$ 1.80	3.99	0.085	3.58	···
PGR J00410+0157	21.75	···	19.02	0.08	14.7	A	$>$ 2.73	4.32	0.018	4.23	···
PGR J00418+0345	21.83	···	17.76	0.04	15.0	A	$>$ 4.07	2.76	0.020	2.66	···
PGR J00434+0704	21.58	···	17.85	0.03	14.6	A	$>$ 3.73	3.25	0.038	3.07	···
PGR J00446+1055	21.73	···	19.33	0.09	14.8	A	$>$ 2.39	4.53	0.061	4.24	···
PGR J00451+1802	21.83	···	18.52	0.06	14.1	A	$>$ 3.31	4.42	0.056	4.15	···
PGR J00515+0021	21.71	···	19.79	0.13	15.9	B	$>$ 1.92	3.89	0.022	3.78	···
PGR J00547+0224	21.64	···	19.26	0.10	14.8	A	$>$ 2.38	4.46	0.029	4.32	···
PGR J00550+0905	22.31	···	19.67	0.11	14.6	A	$>$ 2.63	5.07	0.055	4.81	···
PGR J00577+0631	21.62	···	16.89	0.03	14.1	A	$>$ 4.73	2.79	0.048	2.56	···
PGR J00586+0431	21.53	···	17.13	0.02	14.8	A	$>$ 4.40	2.33	0.024	2.21	···
PGR J00590+1255	21.50	···	19.21	0.09	14.0	D	$>$ 2.30	5.21	0.071	4.87	···
PGR J01010+2230	21.70	···	18.23	0.03	13.0	D	$>$ 3.47	5.23	0.035	5.06	···
PGR J01028+1324	23.21	···	17.95	0.01	13.7	D	$>$ 5.27	4.25	0.035	4.08	MIS
PGR J01048+1639	22.41	···	18.94	0.02	14.2	A	$>$ 3.46	4.75	0.049	4.51	GI
PGR J01051+1624	22.58	···	17.70	0.01	13.5	D	$>$ 4.87	4.20	0.050	3.96	GI
PGR J01109+1845	21.91	···	18.79	0.05	14.5	A	$>$ 3.12	4.29	0.048	4.06	···
PGR J01117+1746	21.72	···	18.78	0.07	14.3	A	$>$ 2.94	4.48	0.077	4.11	···
PGR J01122+1813	21.44	···	17.43	0.03	13.7	D	$>$ 4.01	3.73	0.060	3.44	···
PGR J01135+1845	22.04	···	20.36	0.17	15.0	A	$>$ 1.67	5.36	0.047	5.13	···
PGR J01162+1714	21.53	···	16.70	0.02	12.2	D	$>$ 4.84	4.50	0.071	4.16	···
PGR J01162+1840	21.85	···	18.28	0.05	15.1	A	$>$ 3.57	3.18	0.050	2.94	···
PGR J01369+1653	21.51	···	19.78	0.12	15.2	A	$>$ 1.74	4.58	0.110	4.05	···
PGR J02000+1409	20.62	0.07	15.72	0.01	13.0	D	4.90	2.72	0.053	2.47	MIS
PGR J02040+1500	21.90	0.47	18.74	0.06	14.3	A	3.16	4.44	0.076	4.07	comp?
PGR J02047+1514	22.41	0.14	15.71	0.01	11.6	D	6.70	4.11	0.051	3.87	GI
PGR J02549+1259	21.43	···	19.03	0.08	14.7	A	$>$ 2.40	4.33	0.183	3.45	···
PGR J02561+1257	21.36	···	19.49	0.08	15.5	A	$>$ 1.87	3.99	0.164	3.20	···
PGR J02572+1313	21.52	···	18.96	0.06	14.6	A	$>$ 2.56	4.36	0.148	3.65	···
PGR J03037+1202	21.16	···	18.71	0.07	14.4	A	$>$ 2.45	4.31	0.264	3.04	···
PGR J03130+0313	21.07	···	17.91	0.05	13.5	D	$>$ 3.15	4.41	0.095	3.95	···
PGR J03133+0542	21.37	···	19.30	0.07	14.1	A	$>$ 2.07	5.20	0.233	4.08	···
PGR J03281+0035	21.13	···	17.39	0.04	14.3	A	$>$ 3.75	3.09	0.123	2.50	···
PGR J08237+6750	21.46	0.38	16.48	0.02	13.9	A	4.97	2.58	0.042	2.38	···
PGR J08315+4047	20.84	0.31	15.97	0.02	12.8	A	4.87	3.17	0.039	2.98	···
PGR J08391+4710	22.81	···	17.75	0.01	13.8	A	$>$ 5.07	3.95	0.027	3.82	MIS
PGR J08392+4624	21.51	···	16.62	0.02	13.0	A	$>$ 4.89	3.62	0.026	3.49	···
PGR J08401+4421	20.65	0.23	16.88	0.03	13.2	A	3.77	3.68	0.024	3.57	comp?
PGR J08430+4447	21.33	···	16.24	0.01	12.9	A	$>$ 5.09	3.34	0.026	3.21	···
PGR J08430+4609	20.98	0.28	16.60	0.02	14.1	A	4.39	2.50	0.028	2.37	···

Table 2—Continued

Name	F (mag)	$\sigma(F)$[a] (mag)	N (mag)	$\sigma(N)$ (mag)	V (mag)	Ref[b]	$(F-N)$[a] (mag)	$(N-V)$ (mag)	E$(B-V)$[c] (mag)	$(N-V)_\circ$ (mag)	Remarks
PGR J08431+4606	22.09	···	16.06	0.02	12.4	A	> 6.04	3.65	0.029	3.51	···
PGR J08433+4606	21.00	0.26	16.44	0.02	13.5	A	4.57	2.94	0.029	2.80	···
PGR J08484+2714	21.69	···	18.78	0.06	15.3	B	> 2.92	3.48	0.047	3.25	···
PGR J08538+2708	21.57	···	20.12	0.15	15.3	B	> 1.44	4.82	0.033	4.66	···
PGR J09059+6027	22.87	···	19.83	0.11	16.3	B	> 3.04	3.52	0.035	3.35	···
PGR J09069+5722	22.95	···	18.28	0.01	13.6	B	> 4.67	4.68	0.026	4.55	MIS
PGR J09087+6024	22.90	···	19.91	0.03	15.4	B	> 2.99	4.51	0.039	4.32	NGA
PGR J09165+3213	20.88	0.22	15.40	0.01	12.4	A	5.48	3.00	0.019	2.91	···
PGR J09190+4314	21.68	···	17.13	0.02	14.1	A	> 4.55	3.03	0.014	2.96	···
PGR J09233+5716	22.57	···	17.99	0.01	12.7	A	> 4.57	5.29	0.036	5.12	MIS
PGR J09281+6503	21.94	0.47	16.23	0.01	12.5	C	5.71	3.73	0.062	3.43	···
PGR J09322+5613	21.82	···	17.76	0.04	13.1	A	> 4.06	4.66	0.023	4.55	···
PGR J09343+6347	21.80	···	18.61	0.06	15.4	B	> 3.18	3.21	0.031	3.06	···
PGR J09370+4228	22.27	···	17.38	0.03	13.5	A	> 4.90	3.88	0.013	3.82	···
PGR J09395+6353	21.72	···	20.08	0.13	15.0	B	> 1.64	5.08	0.037	4.90	···
PGR J10170+5439	21.70	···	18.05	0.05	14.1	B	> 3.65	3.95	0.008	3.91	···
PGR J10173+5052	21.14	···	17.61	0.04	14.0	A	> 3.53	3.61	0.010	3.56	···
PGR J10203+3912	22.14	···	17.45	0.02	13.2	A	> 4.69	4.25	0.012	4.19	···
PGR J10273+5758	23.54	···	17.37	0.01	13.4	C	> 6.17	3.97	0.014	3.90	LOCK
PGR J10319+6212	23.40	0.32	17.35	0.01	14.0	B	6.05	3.35	0.014	3.28	GI
PGR J10337+5505	21.58	0.29	15.44	0.01	12.6	A	6.14	2.84	0.008	2.80	···
PGR J10445+5445	22.23	···	18.54	0.06	13.1	A	> 3.69	5.44	0.011	5.39	···
PGR J10453+5824	24.35	0.17	17.79	0.01	13.8	A	6.56	3.99	0.010	3.94	LOCK
PGR J21005+0221	21.70	···	18.99	0.06	15.7	A	> 2.71	3.29	0.098	2.82	···
PGR J21556+0603	21.34	···	17.82	0.04	14.8	A	> 3.52	3.02	0.051	2.78	···
PGR J22172+1900	21.85	···	18.94	0.08	14.8	A	> 2.90	4.14	0.048	3.91	···
PGR J22199+1828	21.51	···	18.33	0.06	14.1	A	> 3.17	4.23	0.046	4.01	···
PGR J22216+1723	21.32	···	18.87	0.08	14.9	A	> 2.44	3.97	0.049	3.73	···
PGR J22247+0827	21.72	···	19.31	0.09	14.4	A	> 2.41	4.91	0.096	4.45	···
PGR J22263+1657	21.35	···	17.89	0.03	15.3	A	> 3.46	2.59	0.058	2.31	···
PGR J22272+1721	21.16	···	17.52	0.04	15.0	A	> 3.64	2.52	0.066	2.20	···
PGR J22311+1648	21.27	···	17.47	0.03	14.8	A	> 3.81	2.66	0.071	2.32	···
PGR J22451+2134	14.47	0.01	14.58	0.01	14.4	A	−0.11	0.18	0.057	−0.09	hot
PGR J22564+2256	21.79	···	18.32	0.06	15.3	A	> 3.47	3.02	0.047	2.79	···
PGR J22572+2215	21.45	···	19.52	0.08	15.2	A	> 1.93	4.32	0.043	4.11	···
PGR J23001+2512	22.17	···	20.16	0.14	14.9	A	> 2.01	5.26	0.107	4.75	···
PGR J23025+2602	15.06	0.01	15.33	0.01	15.1	A	−0.27	0.23	0.075	−0.13	hot
PGR J23038+2731	21.40	···	18.47	0.06	14.7	A	> 2.93	3.77	0.059	3.49	···
PGR J23254+1236	22.01	···	20.26	0.12	15.3	A	> 1.74	4.96	0.065	4.65	···
PGR J23263+0259	21.52	···	19.95	0.14	15.5	A	> 1.57	4.45	0.040	4.26	···
PGR J23445+0204	21.19	···	18.30	0.06	15.7	A	> 2.89	2.60	0.035	2.43	···
PGR J23479+1048	21.20	···	16.71	0.03	13.8	D	> 4.50	2.91	0.051	2.66	···
PGR J23562+2613	21.57	···	18.08	0.04	15.1	A	> 3.49	2.98	0.036	2.81	···

[a]If no error is reported, then the F magnitude is an upper limit — in this case the $(F-N)$ color is also a limit and is preceded by a ">" symbol.

[b]Reference for the adopted V magnitude (see §2.2).

[c]From Schlegel et al. (1998), as returned by the MAST query.

[d]Dereddened $(N-V)$ color, using $\mathrm{E}(N-V) = 4.8 \times \mathrm{E}(B-V)$.

Table 3. Galex and other measurements for known hot subdwarfs.

Name	GALEX Name	F (mag)	N (mag)	V[1] (mag)	E($B-V$) (mag)	$(F-N)_0$ (mag)	$(N-V)_0$ (mag)
PG 0105+276[2]	GALEX J010816.5+275253	13.97	13.72	14.45	0.058	+0.25	−1.00
PG 0212+148	GALEX J021511.2+150005	13.74	13.98	14.45	0.088	−0.23	−0.90
PG 0220+132	GALEX J022338.4+132734	14.08	14.40	14.78	0.122	−0.31	−0.96
TON 349	GALEX J084718.9+230030	13.87	13.92	15.34	0.031	−0.04	−1.57
PG 2335+107	GALEX J233743.8+105627	14.63	14.77	15.55	0.061	−0.13	−1.07
PG 2356+167	GALEX J235925.3+165641	13.63	13.93	14.21	0.044	−0.30	−0.49

[1]V magnitudes from Allard et al. (1994) (PG 0105+276, PG 0212+148, PG 0220+132) and Green et al. (1986) (TON 349); Strömgren y magnitudes from Green et al. (1986) (PG 2335+107) and Wesemael et al. (1992) (PG 2356+167).

[2]Visual double, see §2.2.

Table 4. GALEX and 2MASS Photometry of Selected PGR objects

Name	$(F-N)$ (mag)	$(N-V)_\circ$ (mag)	V (mag)	$(V-K_s)$ (mag)	$(J-H)$ (mag)	$(J-K_s)$ (mag)	Remarks
PGR J00075+0542	-0.25 ± 0.01	$+0.57 \pm 0.05$	13.0 ± 0.05	$+0.7 \pm 0.05$	0.15 ± 0.03	0.18 ± 0.03	hot
PGR J02040+1500	$+3.16 \pm 0.47$	$+4.07 \pm 0.26$	14.3 ± 0.25	$+1.9 \pm 0.25$	0.36 ± 0.04	0.37 ± 0.04	comp?
PGR J08401+4421	$+3.77 \pm 0.23$	$+3.57 \pm 0.25$	13.2 ± 0.25	$+1.6 \pm 0.25$	0.26 ± 0.04	0.34 ± 0.04	comp?
PGR J22451+2134	-0.11 ± 0.01	-0.09 ± 0.25	14.4 ± 0.25	$+2.0 \pm 0.25$	0.40 ± 0.03	0.45 ± 0.03	hot
PGR J23025+2602	-0.27 ± 0.01	-0.13 ± 0.25	15.1 ± 0.25	$+1.6 \pm 0.25$	0.21 ± 0.04	0.27 ± 0.04	hot